HEALTH AND MEDICINE

Dietary thiamine influences L-asparaginase sensitivity in a subset of leukemia cells

Rohiverth Guarecuco[1], Robert T. Williams[1], Lou Baudrier[1], Konnor La[1,2,3], Maria C. Passarelli[4], Naz Ekizoglu[1,5], Mert Mestanoglu[1,5], Hanan Alwaseem[6], Bety Rostandy[6], Justine Fidelin[6], Javier Garcia-Bermudez[1], Henrik Molina[6], Kıvanç Birsoy[1]*

Tumor environment influences anticancer therapy response but which extracellular nutrients affect drug sensitivity is largely unknown. Using functional genomics, we determine modifiers of L-asparaginase (ASNase) response and identify thiamine pyrophosphate kinase 1 as a metabolic dependency under ASNase treatment. While thiamine is generally not limiting for cell proliferation, a DNA-barcode competition assay identifies leukemia cell lines that grow suboptimally under low thiamine and are characterized by low expression of solute carrier family 19 member 2 (SLC19A2), a thiamine transporter. SLC19A2 is necessary for optimal growth and ASNase resistance, when standard medium thiamine is lowered ~100-fold to human plasma concentrations. In addition, humanizing blood thiamine content of mice through diet sensitizes SLC19A2-low leukemia cells to ASNase in vivo. Together, our work reveals that thiamine utilization is a determinant of ASNase response for some cancer cells and that oversupplying vitamins may affect therapeutic response in leukemia.

INTRODUCTION

Nutrient availability in the tumor environment influences the metabolism of cancer cells and may result in dependencies that can be exploited for therapy (*1*, *2*). Deprivation of highly consumed extracellular nutrients in tumors may impose cancer cells to use specific metabolic pathways for proliferation and survival. For instance, low tumor glucose concentrations up-regulate oxidative phosphorylation, an essential adaptation that can be targeted by the biguanide class of drugs (*3*). Similarly, environmental pyruvate and glutamine levels may determine the anaplerotic substrate on which cancer cells rely (*4*). Exogenous modulation of tumor nutrient supply can also alter metabolic programs and, consequently, therapeutic response (*5*). Through effects on one-carbon metabolism, histidine supplementation or dietary methionine restriction sensitizes cancer cells to commonly used chemotherapeutic agents (*6*, *7*). The use of physiological cell culture media has further demonstrated that nutrient environment induces metabolic changes that affect drug sensitivity (*8*). In these recent studies, simply bringing medium concentrations of uric acid and cystine to physiological levels altered cancer cell responses to 5-fluorouracil and CB-839, respectively (*9*, *10*). Together, these examples illustrate the need for further investigation into which nutrients affect therapeutically relevant metabolic pathways. In particular, it is poorly understood whether vitamins, which act as cofactors for many metabolic reactions, can modulate responses to anticancer drugs.

L-asparaginase (ASNase) is a first-line chemotherapeutic for acute lymphoblastic leukemia (ALL) that depletes the amino acid asparagine from blood, thereby targeting leukemia cells that are unable to synthesize sufficient asparagine (*11*, *12*). Major determinants of ASNase sensitivity include basal expression of asparagine synthetase (ASNS), a key enzyme that converts aspartate to asparagine, as well as the capacity to up-regulate ASNS through ZBTB1 (Zinc Finger and BTB domain-containing protein 1) and activating transcription factor 4 (ATF4) (*13*, *14*). Recent work has identified alternative ways of increasing asparagine availability, such as through proteasome degradation (*15*) or aspartate uptake by solute carrier family 1 member 3 (SLC1A3) (*16*). In addition, other cell types can secrete asparagine or its precursors, which ALLs can use, attenuating ASNase cytotoxicity (*17*, *18*). It remains unclear, however, whether extracellular nutrients that are not asparagine precursors can influence sensitivity to ASNase.

Using a CRISPR-Cas9–based genetic screen, here, we interrogated the metabolic determinants of ASNase sensitivity in leukemia. Our analysis pinpointed thiamine pyrophosphate (TPP) kinase 1 (*TPK1*) as essential for proliferation under ASNase treatment. TPK1 converts thiamine to TPP, a cofactor necessary for the activity of the α-ketoglutarate dehydrogenase (AKGDH) complex. In glutamine-anaplerotic leukemia cells, TPP availability enables asparagine synthesis from extracellular glutamine, when asparagine is depleted. We further identified that physiological levels of thiamine do not limit cell proliferation or ASNase response in most cancer cell lines, except for those that have low expression of SLC19A2, a thiamine transporter. These cancer cell lines become sensitive to ASNase when thiamine concentration is lowered to human plasma levels, which is ~100-fold lower than standard culture conditions. Consistent with this observation, a diet that humanizes mouse plasma thiamine levels sensitized leukemia xenografts with endogenously low SLC19A2 to ASNase. Together, our results suggest that *SLC19A2* expression may be a determinant of ASNase response and that supraphysiological thiamine supplementation could potentially ablate such an association. Furthermore, our work provides a proof of concept that using human physiological vitamin levels can alter cancer cell sensitivity to therapies.

RESULTS

Functional genomics identifies metabolic determinants of proliferation under ASNase treatment

To begin to understand how tumor environment affects ASNase response of diverse cancer types, we used a pool of 62 DNA-barcoded cell lines, consisting mainly of hematopoietic and lymphoid cancers,

[1]Laboratory of Metabolic Regulation and Genetics, The Rockefeller University, New York, NY 10065, USA. [2]Tri-Institutional Program in Computational Biology and Medicine, New York, NY 10065, USA. [3]Department of Computational Biology, Cornell University, Ithaca, NY 14853, USA. [4]Laboratory of Systems Cancer Biology, The Rockefeller University, New York, NY 10065, USA. [5]Bahçeşehir University School of Medicine, Istanbul, Turkey. [6]Proteomics Resource Center, The Rockefeller University, New York, NY 10065, USA.
*Corresponding author. Email: kbirsoy@rockefeller.edu

and generated subcutaneous xenografts in mice treated with either ASNase or vehicle (Fig. 1A and fig. S1, A and B). While most cancer cell lines did not respond to ASNase treatment, this competition assay revealed a set of cell lines as strongly sensitive to it. Consistent with previous work (*19*), many of these lines belong to ALLs that express low levels of *ASNS* mRNA (Fig. 1A). Despite the evidence that *ASNS* expression is a reasonable predictor for ASNase response, we found cancer cell lines with high expression of *ASNS* that appeared to have some sensitivity to ASNase treatment in vivo, whereas some with low expression were resistant. Overall, these data suggest that there may be other factors that affect ASNase response.

To further investigate this possibility, we performed metabolism-focused CRISPR-Cas9–based screens in Jurkat, a T-ALL cell line resistant in our in vivo competition assay (Fig. 1B). Consistent with the essential role of asparagine synthesis under asparagine depletion, our screens yielded *ASNS* as the top-scoring gene, with six of eight *ASNS* guides differentially depleted under ASNase treatment (Fig. 1, C and D). In addition to *ASNS*, we noted scoring of tricarboxylic acid (TCA) cycle genes fumarate hydratase and malate dehydrogenase 2 (*MDH2*), as well as glutamic-oxaloacetic transaminase 2 (*GOT2*), highlighting a route to aspartate, the substrate for ASNS and precursor of asparagine (Fig. 1, C to E, and fig. S1C). Furthermore, single-guide RNAs (sgRNAs) targeting *SLC1A5*, the major glutamine transporter, and *SLC25A12*, a mitochondrial glutamate/aspartate exchanger, were also substantially depleted under ASNase treatment (fig. S1C). Since many cancers use glutamine as a major anaplerotic source (*20*), our results confirm that the pathway from glutamine uptake to asparagine synthesis through the oxidative TCA cycle is necessary for maintaining cell proliferation under ASNase treatment (Fig. 1E). The second top-scoring gene in our screens was *TPK1*, for which all eight guides were differentially depleted when we treated cells with ASNase (Fig. 1, C and D). TPK1 is a ubiquitously expressed cytosolic kinase that uses imported thiamine and adenosine triphosphate to produce TPP, the thiamine derivative that serves as a cofactor for many enzymes, including AKGDH in the TCA cycle (*21*). To our surprise, *TPK1*, though predicted to be a cell-essential gene, did not score under standard culture conditions, suggesting the presence of sufficient TPP for proliferation. Given the lack of any previous connection between thiamine metabolism and ASNase response, we next focused on TPK1.

TPP enables de novo asparagine synthesis and proliferation under ASNase treatment

To understand how *TPK1* loss sensitizes leukemia cells to ASNase, we generated CRISPR-Cas9–mediated clonal knockouts (KOs) of *TPK1*, in which TPK1 protein levels were undetectable (Fig. 2A). Unlike in our genetic screening conditions, *TPK1*-null Jurkat cells die in culture unless supplemented with TPP. This suggests that TPP is essential for proliferation and that TPP from other cells with functional TPK1 may have fueled the growth of *TPK1*-null cells during the course of the genetic screens. To determine whether TPP limitation is sufficient to sensitize Jurkat cells to ASNase, we first determined a TPP dose that enabled suboptimal proliferation of *TPK1*-null cells under standard culture conditions (2.5 nM). At this dose, *TPK1*-null cells were substantially more sensitive to ASNase treatment compared to parental controls (Fig. 2B), consistent with our screen results. Overexpressing sgRNA-resistant *TPK1* complementary DNA (cDNA) rescued both TPP dependency and the TPP-dependent ASNase sensitivity of *TPK1*-null cells (fig. S2, A and B). Together, these results show that TPP availability enables proliferation of leukemia cells upon ASNase treatment.

TPP is used as a cofactor by various enzyme complexes, including the AKGDH complex, which catalyzes the oxidative decarboxylation of α-ketoglutarate in the TCA cycle along the pathway from glutamine to asparagine. To directly determine whether de novo asparagine synthesis from glutamine requires TPP, we measured the generation of TCA cycle intermediates, aspartate, and asparagine from uniformly heavy carbon-labeled glutamine ([U-13C]-L-glutamine) (Fig. 2C), in the presence or absence of TPP and asparagine. We performed this in parental and *TPK1*-null Jurkat cells expressing either a vector or *TPK1* cDNA. In asparagine-replete conditions, we did not detect any asparagine labeling, indicating the lack of asparagine synthesis (Fig. 2D). In contrast, when asparagine was absent, ~50% of the asparagine in parental cells, and *TPK1*-null cells supplemented with TPP or expressing *TPK1* cDNA, was derived from oxidative metabolism of [U-13C]-L-glutamine (Fig. 2D), in line with ATF4-mediated up-regulation of ASNS. In the absence of both asparagine and TPP, we observed a substantial decrease in total as well as oxidatively labeled (M + 4) asparagine, aspartate, and malate in *TPK1*-null cells (Fig. 2, D to F). Addition of TPP or expression of *TPK1* cDNA rescued all decreases in these metabolite levels (Fig. 2, D to F). Notably, *TPK1* loss also led to the massive accumulation of total alpha-ketoglutarate (Fig. 2G), despite total levels of the upstream metabolite glutamate being comparable across all conditions (Fig. 2H). Together with the depletion of total metabolites downstream from alpha-ketoglutarate in the absence of TPP, this is consistent with the cofactor role of TPP for the AKGDH complex. Furthermore, in fractional enrichment profiles, TPP limitation decreased oxidatively labeled (M + 4) asparagine (under asparagine depletion), aspartate, and malate (fig. S2, C to E), compared to TPP-replete conditions and to the oxidative labeling (M + 5) seen for alpha-ketoglutarate (fig. S2F). In contrast, we did not observe any change between the fractional enrichment profiles of alpha-ketoglutarate and glutamate (fig. S2, F and G), suggesting that TPP limitation affects glutamine anaplerosis at a point downstream from alpha-ketoglutarate in the TCA cycle. Together, these metabolite profiles were in line with our genetic screen data by highlighting that utilization of glutamine for the oxidative TCA cycle is essential for asparagine synthesis under exogenous asparagine limitation in Jurkat cells. Furthermore, these results suggest that by enabling AKGDH activity in the TCA cycle, TPP allows asparagine synthesis from glutamine under extracellular asparagine depletion.

SLC19A2 expression is a determinant of growth at physiologically relevant thiamine concentrations

Given that thiamine-derived TPP availability enables growth under ASNase treatment, we considered that conventional RPMI 1640 (RPMI) medium provides supraphysiological (3 μM) thiamine levels. This is approximately 100-fold the content of normal human plasma, which ranges from 6.6 to 43 nM (*22*). Building upon the observation that *TPK1*-null cells display increased ASNase sensitivity under limiting TPP concentrations, we explored two questions: first, that physiological thiamine levels may be a growth limitation for a subset of cancer cell lines; and second, that culturing such a subset in limiting thiamine environments may affect ASNase responses. To address the first question, we performed cell line competition assays in RPMI, with and without added thiamine [supplemented with 10% dialyzed fetal bovine serum (FBS)] (Fig. 3A). Notably, the trace thiamine in dialyzed FBS led to ~1 nM total thiamine in culture,

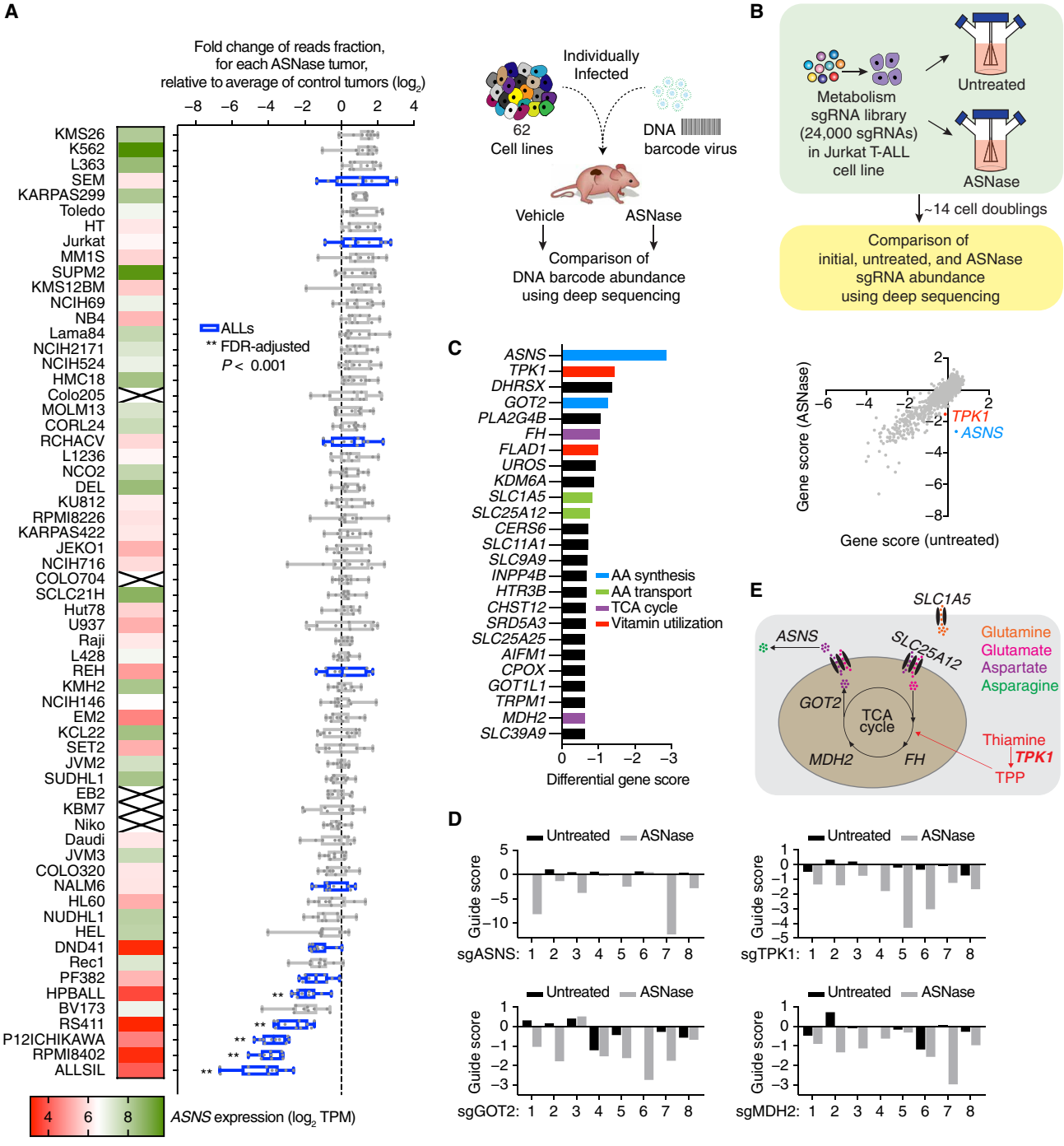

Fig. 1. Functional genomics identifies metabolic determinants of proliferation under ASNase treatment. (**A**) Right: Schematic outlining cell line competition assay. Left: Log_2 fold change in abundance from initial pool, of barcodes ($n = 3$) representing indicated cell lines in the competition assay, for ASNase-treated tumors ($n = 10$) relative to mean of vehicle-treated tumors ($n = 10$). Boxes represent the median and first and third quartiles, and whiskers represent the minimum and maximum of all data points. Statistics: false discovery rate (FDR)–adjusted *P*, by two-tailed unpaired *t* test for unequal variances, of ASNase tumor group versus vehicle tumor group. Individual CCLE RNA-seq *ASNS* expression levels of cell lines are also shown (x indicates no data available). (**B**) Schematic depicting pooled CRISPR screen under ASNase treatment (0.25 U/ml) using a metabolism-focused single-guide RNA (sgRNA) library. (**C**) Left: The top 25 genes differentially required under ASNase treatment are shown. Right: Gene scores for Jurkat cells grown in untreated versus ASNase-treated vessels. Most genes, as well as nontargeting control sgRNAs, gave similar scores in untreated and treated vessels. AA, amino acid. (**D**) Log_2 fold change in the abundance of individual sgRNAs in untreated (black) or ASNase-treated (gray) for top-scoring genes, *ASNS*, *TPK1*, *GOT2*, and *MDH2*. (**E**) Schematic demonstrating that top-scoring genes in the CRISPR screen highlight a specific route from glutamine to asparagine as essential under ASNase treatment.

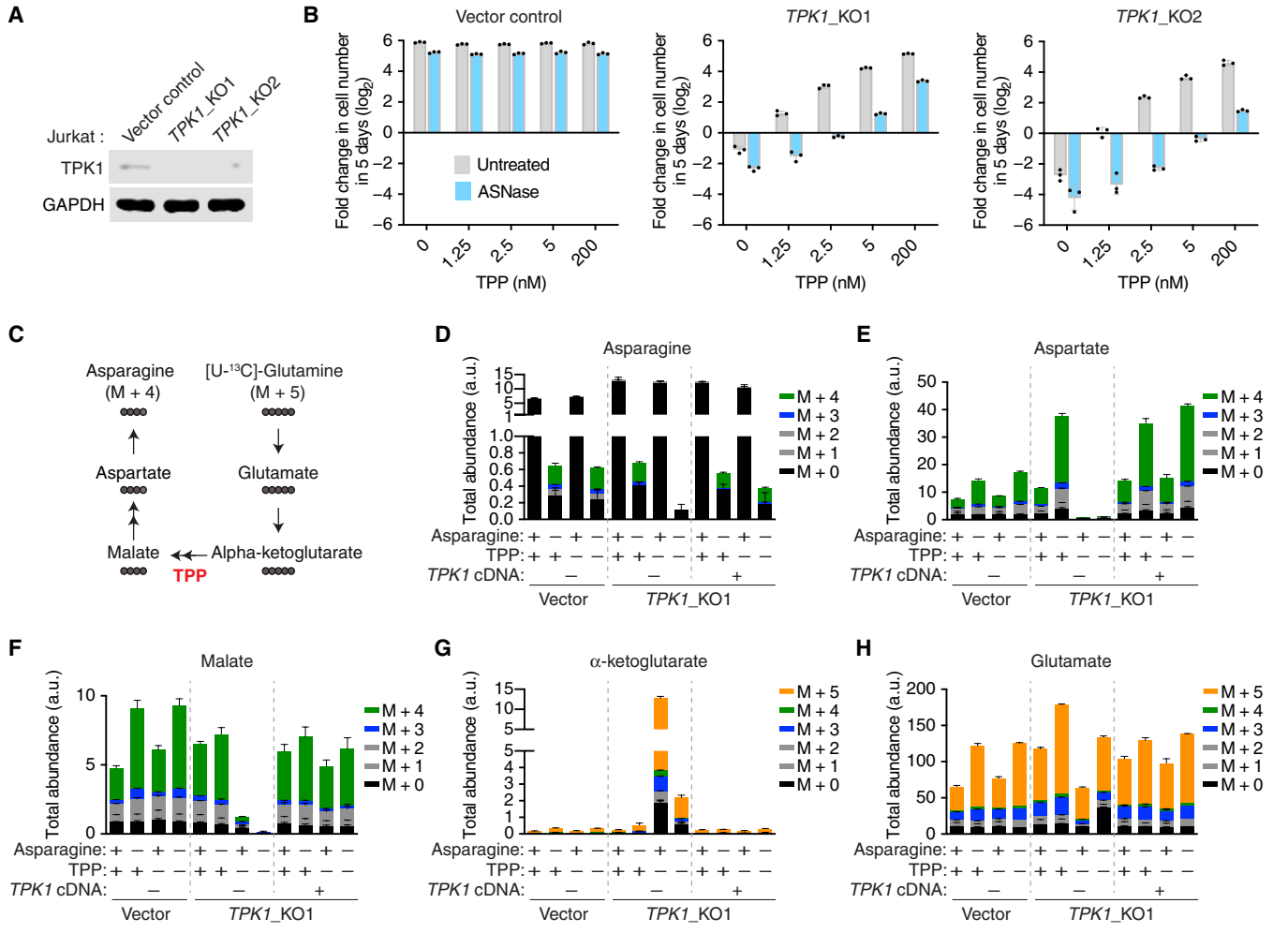

Fig. 2. TPP enables de novo asparagine synthesis and proliferation under ASNase treatment. (**A**) Immunoblot analysis of vector control and two clonal *TPK1* KOs made from Jurkat cells. Glyceraldehyde-3-phosphate dehydrogenase (GAPDH) was used as a loading control. (**B**) Fold change in cell number (log_2) of vector control, *TPK1*_KO1, and *TPK1*_KO2 Jurkat cells, after untreated or 0.0005 U/ml ASNase conditions for 5 days (mean ± SD, $n = 3$). Statistics: $P < 0.05$ by two-tailed unpaired t test for equal variances, for all 15 untreated-treated pairs. (**C**) Schematic depicting a metabolic route of asparagine synthesis from glutamine. Filled circles represent 13C atoms derived from [U-^{13}C]-glutamine. (**D** to **H**) Total abundance [a.u. (arbitrary units)] of indicated metabolites derived from labeled glutamine in vector control, *TPK1*_KO1, and cDNA-rescued *TPK1*_KO1 Jurkat cells. Cells were incubated for 24 hours in medium containing [U-^{13}C]-glutamine (2 mM) in the presence or absence of asparagine (378 μM) and TPP (3 μM). Colors indicate mass isotopologs (mean ± SD, $n = 3$).

which approximated the content of human plasma. While many cancer cell lines grew similarly in both conditions, we observed that a small subset was depleted in the competition assay specifically under low thiamine, suggesting that low thiamine content limited their proliferation. We next determined whether the expression of any particular thiamine metabolism gene is predictive of growth responses to thiamine limitation. Correlating growth in low thiamine with mRNA expression data of metabolic genes from CCLE (Cancer Cell Line Encyclopedia) revealed the plasma membrane thiamine transporter *SLC19A2* as a top-scoring gene (Fig. 3B). Expression of *SLC19A3*, the other canonical thiamine transporter, was not a predictor of growth under low thiamine, and low mRNA levels of *SLC19A3* compared to *SLC19A2* in CCLE (median TPM (transcripts per million) of 0.1 versus 6.6) suggested that *SLC19A2* may be the primary transporter expressed in cancer lines. To further support the competition assay results, we simultaneously performed a metabolism-focused CRISPR-Cas9–based genetic screen using Jurkat cells under the same low- and high-thiamine conditions. Similar to the correlation results from the cell competition assays, *SLC19A2* was the top-scoring gene, with five of eight guides being selectively depleted in low-thiamine medium (Fig. 3, C and D). Notably, additional genes with no known connections to thiamine uptake scored in our screen, suggesting that other metabolic dependencies exist when thiamine is low. Together, our unbiased competition assay and genetic screen approaches both pinpoint that *SLC19A2* expression may be a determinant of growth at physiologically relevant thiamine concentrations. Given the connection between thiamine utilization and ASNase response, we next asked whether cell lines with low SLC19A2 are more sensitive to ASNase under limiting physiological thiamine. To address this, we identified three B-ALL cell lines, KOPN8, REH, and NALM6, in which *SLC19A2* mRNA was undetectable, consistent with CCLE data (Fig. 3E).

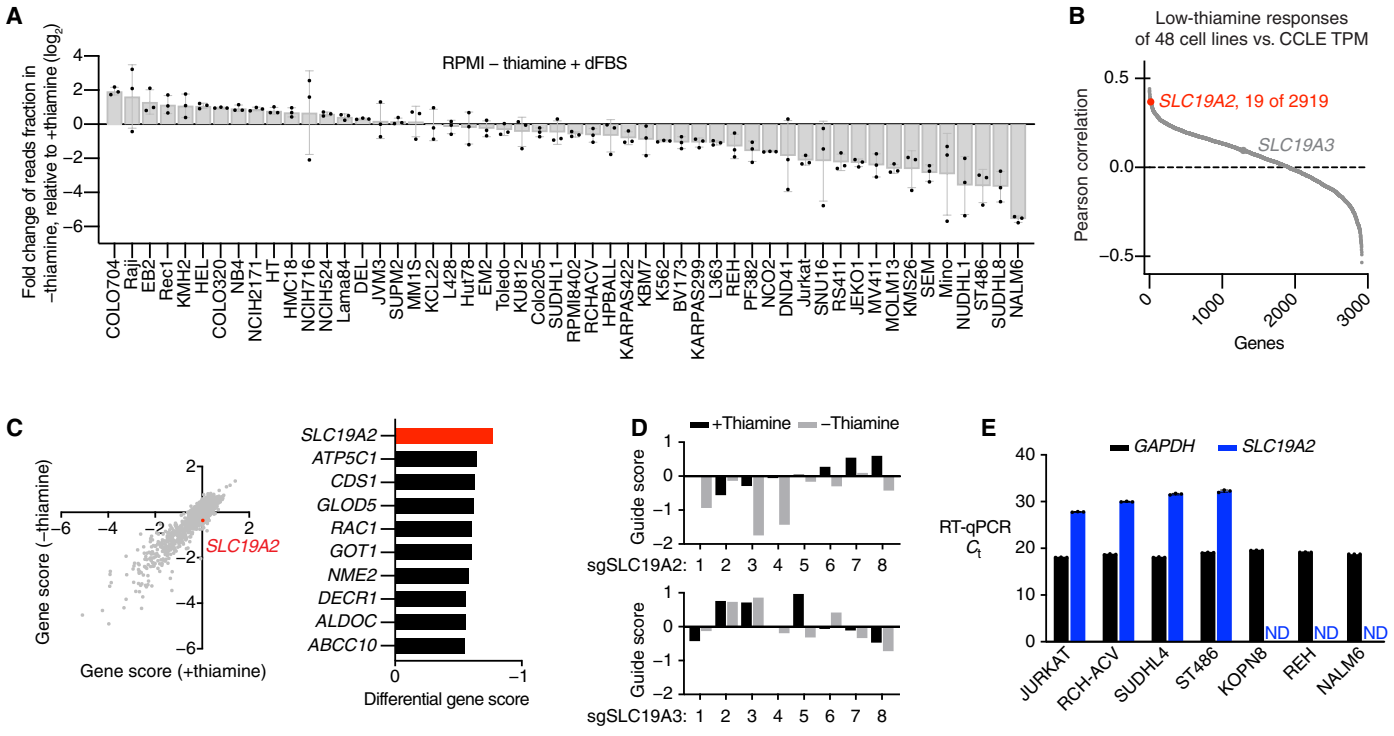

Fig. 3. *SLC19A2* expression is a determinant of growth at physiologically relevant thiamine concentrations. (**A**) Log_2 fold change in abundance since initial pool, of DNA barcodes representing indicated cell lines in a competition assay, for cells grown in the absence of thiamine (–thiamine), relative to growth responses in the presence of 3 μM thiamine (+thiamine) (mean ± SD, $n = 3$ independent barcodes). Media were supplemented with 10% dialyzed FBS (dFBS), which contributes ~1 nM thiamine. (**B**) Low-thiamine cell competition responses were correlated with CCLE mRNA expression data of metabolic genes, and thiamine transporter 1 (*SLC19A2*), but not thiamine transporter 2 (*SLC19A3*), had one of the top-scoring Pearson's correlation coefficients. TPM, transcripts per million. (**C**) Left: Gene scores for a CRISPR screen done with Jurkat cells in the presence (+thiamine) or absence (–thiamine) of 3 μM thiamine. Media were supplemented with 10% dialyzed FBS, which contributes ~1 nM thiamine. Most genes gave similar scores in the two conditions. Right: The top 10 genes differentially required in low thiamine are shown. (**D**) Log_2 fold change in the abundance of individual sgRNAs in our CRISPR screen, in the presence (+thiamine) or absence (–thiamine) of 3 μM thiamine, for *SLC19A2* (top) and *SLC19A3* (bottom). (**E**) Baseline mRNA levels by real-time quantitative polymerase chain reaction (RT-qPCR) of indicated genes for cell lines representing the following cancers: T-ALL (JURKAT), B-ALL (RCH-ACV, KOPN8, REH, and NALM6), diffuse large B cell lymphoma (SUDHL4), and Burkitt lymphoma (ST486). ND, not detected (mean ± SD, $n = 3$).

Physiological thiamine is limiting for ASNase response of SLC19A2-low cells

We had previously noted that REH and NALM6 were ASNase resistant in barcoded competitions in mice, but we considered that the standard mouse chow that we used may have supplied supraphysiological thiamine. Consistent with the in vivo competition results, REH cells proliferated similarly in the presence and absence of ASNase under standard culture conditions (3 μM thiamine). However, under low-thiamine (~60 nM) conditions, untreated cells grew slightly less than at 3 μM (two versus four doublings in 6 days) but now, notably, ASNase treatment severely impaired cell growth (no doublings in 6 days). Furthermore, overexpression of *SLC19A2* was sufficient to rescue both the decreased growth of untreated cells and the increased ASNase response at ~60 nM thiamine (Fig. 4A). This suggests that *SLC19A2* expression is a determinant of both growth and ASNase sensitivity in low thiamine. Consistent with this, as we further lowered thiamine toward 10 to 40 nM to be within the human plasma range, we found that for SLC19A2-low NALM6 and REH cells, thiamine levels constrained growth and ASNase had a greater effect, compared to cells cultured in supraphysiological thiamine (Fig. 4B and fig. S3A). In contrast, SLC19A2-high Jurkat, ST486, and RCH-ACV cells were unaffected by physiological thiamine concentrations, and their ASNase response was similar at high and low thiamine (Fig. 4B and fig. S3B). CRISPR-Cas9–mediated targeting of *SLC19A2* in Jurkat, which decreased 13C-labeled thiamine uptake, showed that *SLC19A2* was necessary for cells to proliferate optimally and maintain ASNase resistance under human plasma thiamine levels relative to cells in standard culture (Fig. 4, C and D). Together, these data establish *SLC19A2* expression as a determinant of (i) growth and (ii) ASNase response at physiological thiamine levels.

Dietary thiamine intake influences ASNase sensitivity of SLC19A2-low leukemia cells in vivo

To confirm that endogenously low expression of *SLC19A2* in cell lines is not a tissue culture phenomenon, we probed for the existence of SLC19A2-low patient tumors. As ASNase is a standard in the initial treatment phase of ALL, we explored RNA sequencing (RNA-seq) data of pediatric primary ALLs sampled from peripheral blood and bone marrow, as well as recurrent ALLs sampled from bone marrow. *ASNS*, *TPK1*, and *SLC19A2* mRNAs were consistently detected in these three datasets (fig. S4A), and their expression was similar between primary and recurrent bone marrow datasets, suggesting that treatment generally did not influence mRNA levels of these genes. Notably, *SLC19A3* mRNA was rarely detected, indicating that SLC19A2 is likely the primary thiamine transporter in these tumors. These data show a diverse range of *SLC19A2* expression among patients and

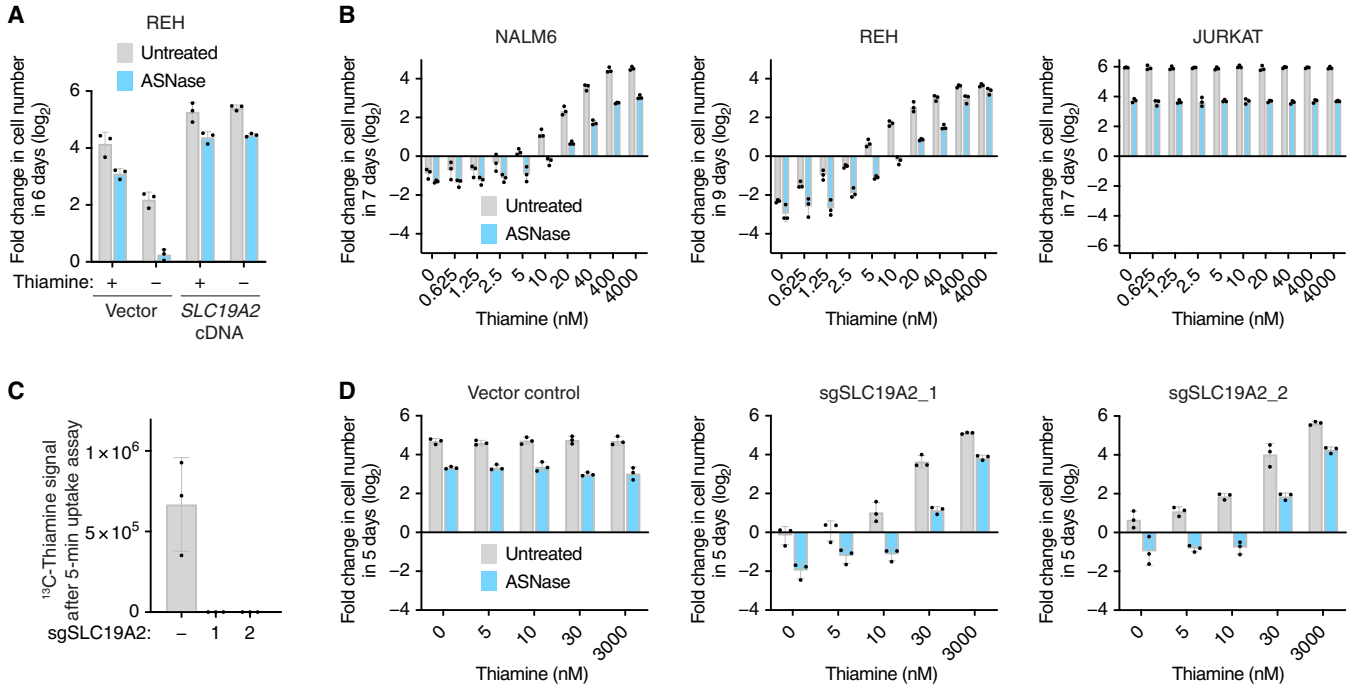

Fig. 4. Physiological thiamine is limiting for ASNase response of SLC19A2-low cells. (**A**) Fold change in cell number (log_2) of vector control and *SLC19A2* cDNA–expressing REH cells, after untreated or 0.001 U/ml ASNase conditions for 6 days, in the presence (+) or absence (–) of 3 μM thiamine (mean ± SD, $n = 3$). Media were supplemented with 10% regular FBS, which contributes ~60 nM thiamine. $P < 0.05$ for all four untreated-treated pairs. (**B**) Fold change in cell number (log_2) of SLC19A2-low (NALM6 and REH) and SLC19A2-high (JURKAT) wild-type cell lines, after untreated or 0.001 U/ml ASNase conditions for 7 to 9 days, at different thiamine concentrations added to thiamine-free RPMI supplemented with 10% double-dialyzed FBS (mean ± SD, $n = 3$). $P < 0.05$ for untreated-treated pairs at these thiamine concentrations: JURKAT, all concentrations; NALM6, all above 1.25 nM; REH, all above 0 nM. (**C**) ^{13}C-thiamine uptake in vector control–, sgSLC19A2_1-, and sgSLC19A2_2-expressing Jurkat cells (mean ± SD, $n = 3$). (**D**) Fold change in cell number (log_2) of vector control–, sgSLC19A2_1-, and sgSLC19A2_2-expressing Jurkat cells, after untreated or 0.001 U/ml ASNase conditions for 5 days, at different thiamine concentrations added to thiamine-free RPMI supplemented with 10% double-dialyzed FBS (mean ± SD, $n = 3$). $P < 0.05$ for all 15 untreated-treated pairs. Statistics for (A), (B), and (D): two-tailed unpaired *t* test for equal variances.

confirm the existence of SLC19A2-low tumors in which ASNase response may depend on environmental thiamine.

We next asked whether extracellular thiamine availability also affects ASNase response of SLC19A2-low leukemia cells in vivo. To create a model of such tumors, we used the SLC19A2-low REH cell line and generated orthotopic tumors in nonobese diabetic severe combined immunodeficiency gamma (NSG) mice. First, mice that were on the conventional chow–based diet used in our barcoded competition experiment were placed on a purified-ingredients diet with either a high thiamine amount to mimic the supraphysiological plasma thiamine levels obtained with chow (Fig. 5A and fig. S4, B to D) or a low amount that resulted in levels resembling that of human serum (Fig. 5A and fig. S4D). Lowering plasma thiamine to human levels was well tolerated, as indicated by animal weights remaining unchanged after diet modification (Fig. 5B). We then engrafted REH cells in mice on either high- or low-thiamine diets and tested the efficacy of ASNase treatment in each of these cohorts. The ASNase regimen depleted plasma asparagine levels without changing the levels of abundant amino acids such as glutamine (fig. S4E). Compared to the high-thiamine diet group in which plasma thiamine was comparable to that seen with standard chow, neither ASNase treatment nor lowering dietary thiamine alone significantly affected survival from leukemia (Fig. 5C). Notably, proliferation of these leukemia cells slowed under low-thiamine conditions in vitro, raising the possibility that the in vivo microenvironment may not contain low enough thiamine to impair growth. However, combining ASNase treatment and low dietary thiamine significantly (Mantel-Cox $P = 0.0034$) extended survival from leukemia (Fig. 5C). Together, our results provide evidence that thiamine availability resulting from dietary intake can affect ASNase sensitivity of SLC19A2-low ALLs in vivo.

DISCUSSION

Our results suggest that extracellular thiamine availability influences ASNase response of a subset of leukemia cells. When combined with a change in dietary thiamine intake, ASNase treatment extends survival in a mouse leukemia model. It is important to note that the low-thiamine dietary intervention was equivalent to maintaining normal human serum levels and was sufficient to sensitize SLC19A2-low leukemia cells to ASNase. Lowering thiamine levels further than the normal physiological range for therapeutic purposes in experimental or clinical settings would likely have adverse consequences, because of the diverse functions of TPP in normal cell types. In addition to its role in the AKGDH complex, TPP serves as a cofactor for various other enzymes, including the pyruvate dehydrogenase (PDH) complex, the branched-chain alpha-ketoacid dehydrogenase complex, and transketolase (*23*). Thus, biochemical abnormalities, such as lactic acidosis resulting from diminished PDH activity, are among the symptoms observed in patients with nutritional thiamine deficiency (*23*–*25*).

Although high thiamine supplementation is warranted in cases of deficiency, prophylactic use has been suggested with limited evidence for other scenarios, including preventing potential side effects of adult

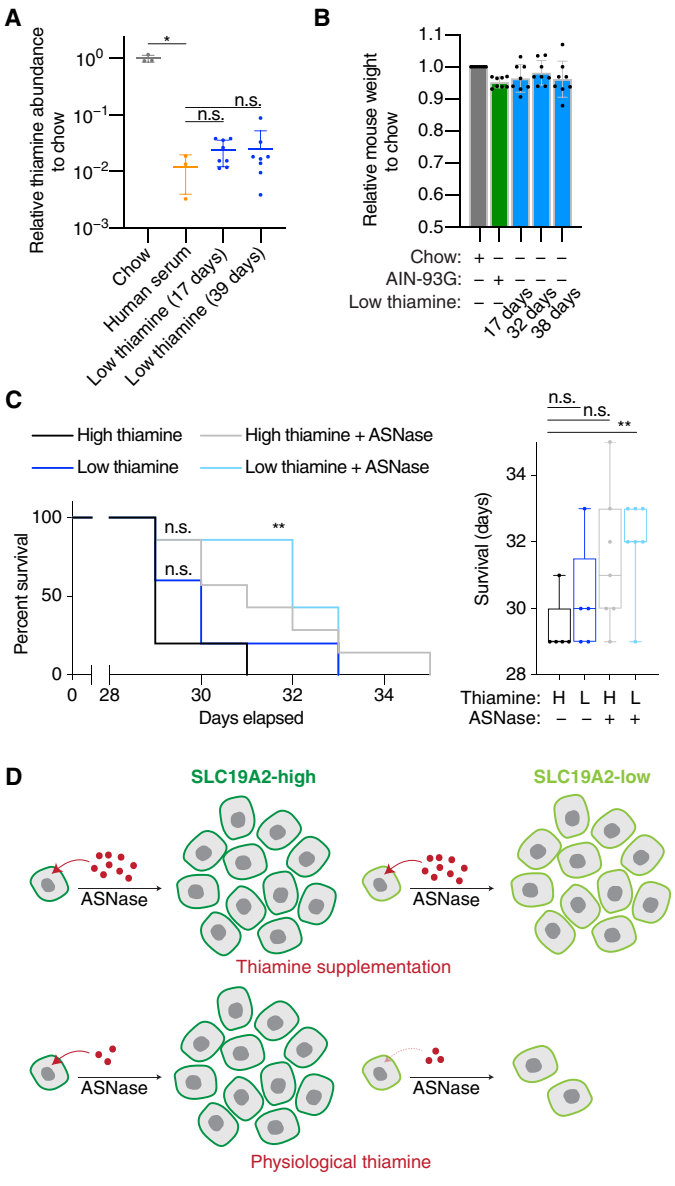

Fig. 5. Dietary thiamine intake influences ASNase sensitivity of SLC19A2-low leukemia cells in vivo. (**A**) Plasma thiamine profiling of mice on conventional chow ($n = 3$ mice), and mice on a modified AIN-93G purified diet of low thiamine content ($n = 8$ mice) (mean ± SD). Human serum was profiled simultaneously for relative comparison. Statistics: *$P < 0.01$ by two-tailed unpaired t test for unequal variances. n.s., not significant. (**B**) Weights of mice initially on conventional chow, then switched to standard AIN-3G purified diet for 1 week, and lastly switched to a modified AIN-93G purified diet of low thiamine content ($n = 8$ mice) for indicated times, relative to initial weights on chow (mean ± SD). (**C**) Left: Kaplan-Meier survival curves of NSG mice on high- or low-thiamine AIN-93G diets engrafted with REH (endogenously low SLC19A2 cell line) by tail vein injection and treated with vehicle or ASNase (1000 U/kg, twice per week). Right: Box-and-whisker plots of survival data. Statistics: Left: n.s., Mantel-Cox $P > 0.05/3$ (Bonferroni correction); right: n.s., two-tailed unpaired t test for equal variances $P > 0.05/3$ (Bonferroni correction). For both analyses, **$P < 0.005$. $n = 5$ mice for untreated groups and $n = 7$ mice for ASNase groups. (**D**) Schematic depicting that environmental thiamine influences ASNase sensitivity of leukemia cells with low *SLC19A2* expression.

ASNase administration (*26*, *27*). Such use in patients with ALL should therefore be weighed with the possibility that excess blood thiamine may negatively affect ASNase response of a subset of cancers. However, human studies are needed to further elucidate the effect of excess thiamine on therapeutic response. To determine whether *SLC19A2* expression is predictive of responses to ASNase-containing regimens and patient survival, it would be necessary to measure patient plasma thiamine levels during treatment since having supraphysiological levels could affect response. Another possibility is to document vitamin supplementation during clinical trials, which has been done for those with antioxidant properties like vitamin E, and their use is now discouraged while undergoing chemotherapy and radiotherapy for various cancers (*28*–*30*). Collectively, our work adds to the growing list of studies available that probe whether excess vitamin supplementation may be detrimental during chemotherapy (*31*). Unfortunately, the lack of clinical reports on this topic has translated to nonuniform physician advice with regard to taking vitamin regimens during cancer treatment (*32*, *33*).

Our work also emphasizes the need to better recapitulate tumor nutrient environment in in vitro studies. Recently, the use of novel cell culture media that better reflect human plasma composition has shed light on how nutrient environment affects therapeutic response (*8*, *9*). However, vitamin levels in these media have remained unchanged from the oversupplemented amounts present in conventional formulations. Our data imply that oversupplementation of vitamins may mask drug responses in a variety of preclinical scenarios such as in vitro screening of drug candidates, as well as in vivo validation of novel therapies.

In summary, we uncovered that lowering thiamine to human physiological levels in culture media and in mouse plasma through diet increases the response of a subset of cancer cell lines to ASNase, an important chemotherapeutic in the treatment of ALL (Fig. 5D). This subset is defined by low expression of SLC19A2, the primary thiamine transporter in ALL tumor samples. These results raise the possibility that low *SLC19A2* expression may be associated with greater patient response to ASNase. However, increasing blood thiamine concentrations through excess supplementation could diminish ASNase efficacy in these cancers. In conclusion, our work provides a proof of principle that humanizing the vitamin levels of both in vitro and in vivo models can affect therapeutic sensitivity of cancers that have specific vitamin utilization deficiencies.

MATERIALS AND METHODS

Experimental design

This study was designed to investigate the metabolic determinants of leukemia cell response to ASNase treatment. To address this objective, we (i) performed unbiased genetic screens to find genes that are essential for proliferation under ASNase treatment; (ii) used loss-of-function studies and metabolite profiling to validate that *TPK1* enables ASNase resistance by producing the cofactor TPP, which allows asparagine synthesis in glutamine-anaplerotic leukemia cells; (iii) used a DNA-barcoded cell line competition assay, a genetic screen, and gain- and loss-of-function studies to identify that physiological thiamine is limiting for ASNase response of a subset of leukemia cell lines with low expression of the thiamine transporter SLC19A2; and (iv) orthotopically engrafted leukemia cells with endogenously low SLC19A2 in NSG mice to show that dietary thiamine can influence ASNase sensitivity in leukemia.

Compounds, cell lines, cell culture, and constructs

Antibodies to glyceraldehyde-3-phosphate dehydrogenase (GAPDH) (GTX627408) were from GeneTex, and to TPK1 from Proteintech (10942-1-AP). Conjugated donkey anti-mouse IRDye 680LT and donkey anti-rabbit IRDye 800CW were from LI-COR Biosciences.

Asparagine, TPP, human serum, polybrene, and puromycin were from Sigma-Aldrich; blasticidin from Invivogen; D-glucose from VWR; L-glutamine from Gibco; thiamine hydrochloride from MP Biomedicals; *Escherichia coli* L-asparaginase from BioVendor.

For glutamine tracing, a powder base medium of RPMI without amino acids (R9010-01, US Biological) was supplemented with all individual amino acids (except for asparagine and glutamine) and glucose at RPMI concentrations. [U-^{13}C]-glutamine [CLM-1822-H, Cambridge Isotope Laboratories (CIL)] was used for tracing, and asparagine was present or absent at RPMI concentration as detailed in experiment discussion. For thiamine uptake experiments, thiamine-(4-methyl-^{13}C-thiazol-5-yl-$^{13}C_3$) hydrochloride ("^{13}C-thiamine," 731188, Sigma-Aldrich) was added to cells in Hank's balanced salt solution (HBSS) containing calcium chloride and magnesium chloride (24020-117, Gibco). In tracing, uptake, and plasma profiling experiments, extraction solvents contained ^{15}N and ^{13}C fully labeled internal amino acid standards (MSK-A2-1.2, CIL) for normalization.

All human cell lines used were originally purchased from American Type Culture Collection or German Collection of Microorganisms and Cell Cultures (DZMZ) or obtained from the Sabatini and Weinberg laboratories (Whitehead Institute). Cell lines were verified to be free of mycoplasma and authenticated by short tandem repeat profiling. Cell lines were typically maintained in "standard RPMI": RPMI 1640 medium containing 2 mM glutamine (Gibco), 10% FBS (Sigma-Aldrich) and penicillin-streptomycin (Gibco), at 37°C and 5% CO_2, unless otherwise noted. For all experiments, cells were counted with a Beckman Z2 Coulter Counter.

The DNA-barcoded cell line competition assay and CRISPR-based screen done in low-thiamine medium used thiamine-free RPMIs supplemented with 10% dialyzed FBS (26400044, Gibco). All thiamine-free RPMIs were made with glucose and glutamine at standard RPMI concentrations (11 and 2 mM, respectively). For the competition assay, a powder base medium of RPMI without vitamins (US Biological) was supplemented with all individual vitamins (except for thiamine) at RPMI concentrations. The CRISPR screen used a different powder base medium of RPMI made without thiamine (R9011-01, US Biological), which was used for all other experiments that used thiamine-free RPMI.

For manipulating thiamine levels in the REH EV and *SLC19A2* OE experiments, thiamine-free RPMI was combined with 10% non-dialyzed FBS. For achieving nanomolar thiamine levels that approximated physiological thiamine, thiamine-free RPMI was combined with 10% "double-dialyzed FBS," obtained by further in-house dialysis of Gibco's dialyzed FBS. In-house dialysis was performed at 4°C against a 20× volume of phosphate-buffered saline (PBS), using regenerated cellulose dialysis tubing (21-152-9, Fisherbrand), with a PBS change done after at least 8 hours of stirring, such that four total PBS volumes were spent.

Lentiviral sgTPK1 vector was generated via ligation of hybridized oligos (below) into lentiCRISPR-v2-puro, and lentiviral sgSLC19A2 vector was generated similarly (oligos below) but using lentiCRISPR-v1-RFP (red fluorescent protein). Both of these vectors were linearized with Bsm BI (New England BioLabs), and nonlinearized vectors were used for vector controls. sgRNA-resistant *TPK1*, or *SLC19A2*, cDNA gene blocks were cloned into pMXs-IRES-blast by Gibson assembly, and an uncut vector was used as vector control.

Guide 5 in CRISPR-Cas9 screen, used to generate clonal KO1 and KO2 in proliferation assays:

sgTPK1_5F, 5′-caccGGTGATATCATATAAGCGGT-3′;
sgTPK1_5R, 5′-aaacACCGCTTATATGATATCACC-3′.

Guide 3 in CRISPR-Cas9 screen, referred to as sgSLC19A2_1 in proliferation assays:

sgSLC19A2_3F, 5′-caccGAGGCTGGCGAAGAAGCCGT-3′;
sgSLC19A2_3R, 5′-aaacACGGCTTCTTCGCCAGCCTC-3′.

Guide 4 in CRISPR-Cas9 screen, referred to as sgSLC19A2_2 in proliferation assays:

sgSLC19A2_4F, 5′-caccGGACAAGAACCTGACCGAGA-3′;
sgSLC19A2_4R, 5′-aaacTCTCGGTCAGGTTCTTGTCC-3′.

Generation of KO and cDNA overexpression cell lines

Lentiviral sgTPK1 and sgSLC19A2 vectors generated as described above were transfected into human embryonic kidney (HEK) 293T cells with lentiviral packaging vectors vesicular stomatitis virus glycoprotein (VSV-G) and delta-viral protein R (dVPR). For the overexpression of *TPK1* or *SLC19A2*, retroviral vector with cDNA generated as above was transfected into HEK293T cells with retroviral packaging vectors Gag-pol and VSV-G. X-tremeGENE reagent (Roche) was used for transfection. After 24 hours, cells were given fresh media. Forty-eight hours after transfection, virus-containing medium supernatants were filtered through a 0.45-μm filter to eliminate cells. Cells to be transduced were plated in six-well tissue culture plates with appropriate virus and polybrene (8 mg/ml). Cells were then spin-infected by plate centrifugation at 1100*g* for 1.5 hours at 32°C. After 24 hours, cells were given fresh media. At least 48 hours after infection, transduced cells were selected with puromycin or blasticidin or by bulk-sorting on a BD FACSAria (same gating for all samples, resulting in top 3 to 6% of RFP$^+$ cells). Clonal *TPK1*-KO cells were generated from a single cell isolated by serial dilution of transduced cells into a 96-well plate, in 0.2 ml of 100 μM TPP-supplemented standard RPMI. Single-cell clones were grown for ~3 weeks, and the resultant clones were evaluated for *TPK1* KO by immunoblotting. *TPK1* KOs were then maintained in standard RPMI containing 20 nM TPP, as were the relevant vector control and cDNA-add-back controls, for at least 1 week before proliferation assays. Mixed-population cells transduced with sgSLC19A2s or vector control were maintained in standard RPMI, as this already oversupplements thiamine at 3 μM. Notably, REH and Jurkat cells expressing a luciferase reporter construct were used for generating the vector- or *SLC19A2*-overexpression pair, and the vector-, sgSLC19A2_1-, or sgSLC19A2_2-expressing lines, respectively.

Immunoblotting

Cells were first collected by centrifugation at 300*g* for 4 min and washed twice with PBS. For blotting TPK1, cells were then lysed in cold radioimmunoprecipitation assay (RIPA) buffer [20 mM tris-Cl (pH 7.5), 150 mM NaCl, 1 mM EDTA, 1% Triton X-100, 0.1% SDS, and 0.5% sodium deoxycholate] supplemented with protease inhibitors (Roche) for 5 min on ice. Supernatants were then collected by centrifugation at 20,000*g* for 8 min at 4°C, and protein concentration was determined using the Pierce BCA Protein Assay Kit (Thermo Fisher Scientific) with a bovine serum albumin protein standard series. Samples were resolved on 12% SDS–polyacrylamide gel electrophoresis gels and analyzed by immunoblotting using antibodies listed above and a LI-COR Odyssey CLx Imaging System coupled with Image Studio Lite.

RNA extraction, reverse transcription, and real-time quantitative polymerase chain reaction

RNA was extracted using the QIAGEN RNeasy Mini Kit, and 1 μg of RNA was reverse-transcribed using the SuperScript III Reverse Transcriptase Kit (Invitrogen), both according to the manufacturer's instructions. Real-time quantitative polymerase chain reaction (PCR) (qPCR) was performed using SYBR Green PCR Master Mix (Applied Biosystems), and *GAPDH* was used as a housekeeping control. qPCR primer sequences were as follows:

GAPDH forward, 5′-TTGGTATCGTGGAAGGACTC-3′;
GAPDH reverse, 5′-ACAGTCTTCTGGGTGGCAGT-3′;
SLC19A2 forward, 5′-GGCCGGACAAGAACCTGAC-3′;
SLC19A2 reverse, 5′-ACACAGGAAACAGTAGCACCA-3′.

Proliferation assays

Cells were plated in 96-well plates at 1000 cells per well in triplicate in a final volume of 0.2 ml in indicated media and treatments. After 5 to 9 days of growth (depending on proliferation rate), 40 μl of CellTiter-Glo reagent (Promega) was added, and luminescence was read on a SpectraMax M3 plate reader (Molecular Devices). For each experiment, cells were also plated in triplicate in untreated medium for an initial luminescence time point for normalization. For each well, fold change in luminescence was calculated and reported on a $\log_2$ scale. In all proliferation assays, we used an ASNase dose ≤ 0.001 U/ml, which is a dose previously shown to deplete asparagine in medium within 24 hours, without affecting glutamine levels (*34*). In assays that required achieving low thiamine levels, cells were first preincubated for 5 to 9 days in the same low-thiamine-base medium that was subsequently used for plating proliferation assays. Proliferation assays were plated multiple times within this preincubation period with similarly reproduced results.

Mouse studies

Animal studies were conducted according to a protocol approved by the Institutional Animal Care and Use Committee at the Rockefeller University. All experiments used age- and gender-matched NSG mice that were maintained on a standard light-dark cycle, with food and water provided ad libitum. Subcutaneous xenograft tumors for DNA-barcoded competition assays were initiated by injecting 1.5 million of the pooled cells in 100 μl of Dulbecco's Modified Eagle Medium (Gibco) with 30% Matrigel (Corning), once on each mouse flank. These mice were fed 5B1Q (TestDiet), a chow-based diet. Leukemia xenografts were initiated by injecting 750,000 REH cells in 100 μl of PBS through the tail vein. Two weeks before tail vein injections, these mice were switched from 5B1Q to a purified diet of thiamine-deficient AIN-93G pellets (Dyets Inc.) coupled with high or low thiamine supplementation in water as described below. One week before tail veins, REH cells were switched from standard RPMI to a low-thiamine medium (thiamine-free RPMI and dialyzed FBS) to remove excess thiamine from cells. To determine survival after leukemia engraftment, weights were first checked weekly. After the first signs of progressive disease, mice were monitored daily for deaths or signs of end point, and weights were taken at a minimum of twice weekly. Humane end points were (i) 20% weight loss from initial weight and (ii) other obvious signs of disease such as hindlimb dysfunction or notable distress.

Low-thiamine groups were maintained by combining thiamine-deficient AIN-93G pellets with water bottles containing 5 μM thiamine. High-thiamine groups were maintained by combining the same thiamine-deficient pellets with 125 μM thiamine in water. Mice were treated with L-asparaginase (1000 U/kg) daily for cell competition assays (2 weeks) and twice weekly for leukemia xenograft experiments (~4 weeks). For all plasma profiling, whole blood was collected using EDTA-coated capillaries or tubes by tail clip (except for the 39-day time point in Fig. 5A and for fig. S4B, for which submandibular bleeds were done) and then centrifuged at 20,000*g* for 5 min at 4°C to yield the plasma supernatants used for liquid chromatography–mass spectrometry (LC-MS) analysis.

Metabolite profiling: Isotope tracing, isotope uptake, and plasma profiling

For glutamine tracing, the three cell types were first taken from their maintenance medium (20 nM TPP) and washed twice with PBS. Cells were then plated at 500,000 cells/ml in medium containing 2.5 nM TPP, for ~1 day, to begin TPP depletion. To begin the experiment, cells were washed again and then plated in triplicate per condition in six-well plates at 1 million cells/ml, in a custom RPMI (described above) containing no asparagine, no TPP, and 2 mM [U-^{13}C]-glutamine (supplemented with 10% dialyzed FBS). TPP (at RPMI thiamine concentration) and asparagine (at RPMI concentration) were then added to wells as appropriate. After 24 hours, 1 million cells from each well were washed twice with 1 ml of cold 0.9% NaCl; a separate tube of 1 M cells was also processed for each experimental condition to check protein content. After washing, polar metabolites were extracted in 1 ml of cold 80% methanol containing internal amino acid standards, by vortexing for 10 min at 4°C. Samples were then centrifuged at 20,000*g* for 15 min at 4°C, and 900 μl of supernatants was stored overnight at −80°C and then nitrogen-dried. Dried extracts were kept at −80°C until LC-MS analysis. Dried samples were resuspended in 100 μl of 50:50 acetonitrile:water, and 2 μl was injected onto the LC-MS column. For protein quantification, NaCl-washed cell pellets were instead stored at −20°C until RIPA lysis and protein quantification (as described above for TPK1 immunoblotting).

For thiamine uptake experiments, the three cell types were first taken from their maintenance in standard RPMI and washed twice with PBS. Four million cells were then plated in triplicate per condition in six-well plates at 1 million cells/ml in warm HBSS. ^{13}C-thiamine was then added to wells at a final concentration of 25 nM, for 5-min incubations at 37°C. The assay was stopped by pipetting each well into an ice-cold tube of HBSS containing unlabeled thiamine that came to 3 μM in the final mixture. Cells were then washed twice with cold 0.9% NaCl and processed as described above for polar metabolite extraction and LC-MS analysis. Dried samples were resuspended in 60 μl of 50:50 acetonitrile:water, and 5 μl was injected onto the LC-MS column.

For plasma profiling, polar metabolites were extracted by combining plasma with cold 75:25 acetonitrile:methanol containing internal amino acid standards. Plasma (5 μl) was combined with either 45 μl of solvent for the in vivo competition assay data or with 20 μl of solvent for custom thiamine diet experiments (for quantifying low-abundance thiamine in plasma). This was followed by vortexing for 5 min at 4°C and then centrifuging at 20,000*g* for 10 min at 4°C. Supernatants were taken immediately for LC-MS analysis or first stored at −80°C for no longer than 24 hours (samples were never dried). Two microliters (for competition assay) or 5 μl (for custom thiamine diet experiments) was injected directly onto the LC-MS column.

LC-MS analysis was conducted on a Q Exactive benchtop Orbitrap mass spectrometer equipped with an Ion Max source and a

HESI II probe, which was coupled to a Vanquish UHPLC system (Thermo Fisher Scientific). External mass calibration was performed using the standard calibration mixture every 4 to 6 days. Samples were injected onto a ZIC-pHILIC 150 × 2.1 mm (5-μm particle size) column (EMD Millipore). Chromatographic separation was achieved using the following conditions: Buffer A was 20 mM ammonium carbonate, 0.1% ammonium hydroxide; buffer B was acetonitrile. The pH for buffer was adjusted to 9.3 using formic acid. The column oven and autosampler tray were held at 25° and 4°C, respectively. The chromatographic gradient was run at a flow rate of 0.150 ml/min as follows: 0 to 22 min: gradient from 90 to 40% B; 22 to 24 min: held at 40% B; 24 to 24.1 min: return to 90% B; 24.1 to 30 min: hold at 90% B. The mass spectrometer was operated in a full-scan, polarity-switching mode with the spray voltage set to 3.0 kV, the heated capillary was held at 275°C, and the HESI probe was held at 250°C. The sheath gas flow was set to 40 U; the auxiliary gas flow was set to 15 U. The MS data acquisition was performed in a range of 55 to 825 mass/charge ratio, with the resolution set at 70,000, the AGC (automatic gain control) target at 10×10^6, and the maximum injection time at 80 ms. Relative quantitation of polar metabolites was performed with Skyline Daily from MacCoss Lab Software (*35*), using a 2-parts-per-million mass tolerance and referencing an in-house library of chemical standards. For normalization, raw signal of each metabolite was first normalized to the appropriate labeled internal amino acid standard in that injection (except for the thiamine uptake data, where raw signal is presented because no signal was detected in sgSLC19A2 samples). Metabolite levels were also normalized by cell counting (per well) and by protein content (per condition, quantified by BCA Protein Assay) for glutamine tracing, by cell counting for thiamine uptake, and by plasma/serum volume as appropriate.

CRISPR-Cas9–based genetic screens

The metabolism-focused sgRNA library preparation and details on performing screens were previously described (*36*–*38*). sgRNA oligonucleotides were synthesized by Agilent and amplified by PCR. After Illumina deep sequencing of initial and final screen pools, a guide score for each screen flask was defined as the $\log_2$ fold change of sgRNA abundance from initial to final. Gene scores for each flask were defined as the median of the guide scores corresponding to a gene, and the complete lists of gene scores were used to make the gene score versus gene score linearity plots presented. For each sgRNA of a gene, the guide score for the control flask was subtracted from the guide score for the experimental flask, and the median of the resulting values was defined as the differential gene score. A gene lethality cutoff was used for differential gene score analysis: Genes that had a gene score less than or equal to −1 in the appropriate control condition were removed from the gene score list, and the updated gene list was ranked by differential gene score of experimental versus control to give the differential gene score graphs presented. Full screen results are available as supplementary data.

DNA-barcoded cell line competition assays

DNA-barcoded cell lines were generated, and competition assays were performed, as previously described (*3*, *39*). In brief, three unique seven–base pair sequences were transduced into each cancer cell line using lentiviruses generated with pLKO.1-puro vector, such that each cell line had three data points used for statistical analysis. To perform cell competition assays, barcoded cell lines were mixed in approximately equal amounts, an initial pool sample was taken, and the remainder of the pool was grown for ~2 weeks under indicated in vitro or in vivo conditions. At end point, genomic DNA was extracted from the initial and final pool samples, DNA barcode regions were amplified by PCR, and PCR amplicons were processed for Illumina deep sequencing. Fold change of barcode abundance from initial to final pools was determined, and results are presented as detailed in appropriate figures.

Patient tumor and cell line RNA-seq

Patient RNA-seq data for *SLC19A2*, *SLC19A3*, *TPK1*, and *ASNS* were generated by the Therapeutically Applicable Research to Generate Effective Treatments (https://ocg.cancer.gov/programs/target) initiative, phs000218. These data were part of the Acute Lymphoblastic Leukemia (ALL) Expansion Phase 2 TARGET substudy, phs000464, and were downloaded from the TARGET Data Matrix (https://ocg.cancer.gov/programs/target/data-matrix) on 10 December 2019. All files used were in the BCCA (British Columbia Cancer Agency) subdirectory, and tumor sample details are indicated within the relevant figures. Cancer cell line RNA-seq data presented throughout this study were obtained from the CCLE (https://portals.broadinstitute.org/ccle/data), accessed on 27 January 2020 (file version: CCLE_RNAseq_rsem:genes_tpm:20180929.txt.gz) (*40*).

Statistical analysis

Significance *P* values, sample sizes, and means are indicated in text or figures. Error bars represent SD from biological replicates or independent samples as indicated. Statistical analyses were performed with GraphPad Prism or Microsoft Excel as appropriate. $P \leq 0.05$ was considered statistically significant, and the specific statistical test used and any adjustments for multiple comparisons are indicated in the relevant figure legends.

SUPPLEMENTARY MATERIALS

Supplementary material for this article is available at http://advances.sciencemag.org/cgi/content/full/6/41/eabc7120/DC1

View/request a protocol for this paper from *Bio-protocol*.

REFERENCES AND NOTES

1. J. Garcia-Bermudez, R. T. Williams, R. Guarecuco, K. Birsoy, Targeting extracellular nutrient dependencies of cancer cells. *Mol. Metab.* **33**, 67–82 (2020).
2. A. Muir, M. G. Vander Heiden, The nutrient environment affects therapy. *Science* **360**, 962–963 (2018).
3. K. Birsoy, R. Possemato, F. K. Lorbeer, E. C. Bayraktar, P. Thiru, B. Yucel, T. Wang, W. W. Chen, C. B. Clish, D. M. Sabatini, Metabolic determinants of cancer cell sensitivity to glucose limitation and biguanides. *Nature* **508**, 108–112 (2014).
4. S. Christen, D. Lorendeau, R. Schmieder, D. Broekaert, K. Metzger, K. Veys, I. Elia, J. M. Buescher, M. F. Orth, S. M. Davidson, T. G. Grünewald, K. De Bock, S.-M. Fendt, Breast cancer-derived lung metastases show increased pyruvate carboxylase-dependent anaplerosis. *Cell Rep.* **17**, 837–848 (2016).
5. N. Kanarek, B. Petrova, D. M. Sabatini, Dietary modifications for enhanced cancer therapy. *Nature* **579**, 507–517 (2020).
6. N. Kanarek, H. R. Keys, J. R. Cantor, C. A. Lewis, S. H. Chan, T. Kunchok, M. Abu-Remaileh, E. Freinkman, L. D. Schweitzer, D. M. Sabatini, Histidine catabolism is a major determinant of methotrexate sensitivity. *Nature* **559**, 632–636 (2018).
7. X. Gao, S. M. Sanderson, Z. Dai, M. A. Reid, D. E. Cooper, M. Lu, J. P. Richie Jr., A. Ciccarella, A. Calcagnotto, P. G. Mikhael, S. J. Mentch, J. Liu, G. Ables, D. G. Kirsch, D. S. Hsu, S. N. Nichenametla, J. W. Locasale, Dietary methionine influences therapy in mouse cancer models and alters human metabolism. *Nature* **572**, 397–401 (2019).
8. T. Ackermann, S. Tardito, Cell culture medium formulation and its implications in cancer metabolism. *Trends Cancer* **5**, 329–332 (2019).
9. J. R. Cantor, M. Abu-Remaileh, N. Kanarek, E. Freinkman, X. Gao, A. Louissaint Jr., C. A. Lewis, D. M. Sabatini, Physiologic medium rewires cellular metabolism and reveals uric acid as an endogenous inhibitor of UMP synthase. *Cell* **169**, 258–272.e17 (2017).

10. A. Muir, L. V. Danai, D. Y. Gui, C. Y. Waingarten, C. A. Lewis, M. G. Vander Heiden, Environmental cystine drives glutamine anaplerosis and sensitizes cancer cells to glutaminase inhibition. *eLife* **6**, e27713 (2017).
11. A. M. Aslanian, B. S. Fletcher, M. S. Kilberg, Asparagine synthetase expression alone is sufficient to induce L-asparaginase resistance in MOLT-4 human leukaemia cells. *Biochem. J.* **357**, 321–328 (2001).
12. P. L. Lorenzi, W. C. Reinhold, M. Rudelius, M. Gunsior, U. Shankavaram, K. J. Bussey, U. Scherf, G. S. Eichler, S. E. Martin, K. Chin, J. W. Gray, E. C. Kohn, I. D. Horak, D. D. Von Hoff, M. Raffeld, P. K. Goldsmith, N. J. Caplen, J. N. Weinstein, Asparagine synthetase as a causal, predictive biomarker for L-asparaginase activity in ovarian cancer cells. *Mol. Cancer Ther.* **5**, 2613–2623 (2006).
13. I. Hermanova, M. Zaliova, J. Trka, J. Starkova, Low expression of asparagine synthetase in lymphoid blasts precludes its role in sensitivity to L-asparaginase. *Exp. Hematol.* **40**, 657–665 (2012).
14. R. T. Williams, R. Guarecuco, L. A. Gates, D. Barrows, M. C. Passarelli, B. Carey, L. Baudrier, S. Jeewajee, K. La, B. Prizer, S. Malik, J. Garcia-Bermudez, X. G. Zhu, J. Cantor, H. Molina, T. Carroll, R. G. Roeder, O. Abdel-Wahab, C. D. Allis, K. Birsoy, ZBTB1 regulates asparagine synthesis and leukemia cell response to L-asparaginase. *Cell Metab.* **31**, 852–861.e6 (2020).
15. L. Hinze, M. Pfirrmann, S. Karim, J. Degar, C. McGuckin, D. Vinjamur, J. Sacher, K. E. Stevenson, D. S. Neuberg, E. Orellana, M. Stanulla, R. I. Gregory, D. E. Bauer, F. F. Wagner, K. Stegmaier, A. Gutierrez, Synthetic lethality of Wnt pathway activation and asparaginase in drug-resistant acute leukemias. *Cancer Cell* **35**, 664–676.e7 (2019).
16. J. Sun, R. Nagel, E. A. Zaal, A. P. Ugalde, R. Han, N. Proost, J.-Y. Song, A. Pataskar, A. Burylo, H. G. Fu, G. J. Poelarends, M. van de Ven, O. van Tellingen, C. R. Berkers, R. Agami, SLC1A3 contributes to L-asparaginase resistance in solid tumors. *EMBO J.* **38**, e102147 (2019).
17. S. Iwamoto, K. Mihara, J. R. Downing, C.-H. Pui, D. Campana, Mesenchymal cells regulate the response of acute lymphoblastic leukemia cells to asparaginase. *J. Clin. Invest.* **117**, 1049–1057 (2007).
18. E. A. Ehsanipour, X. Sheng, J. W. Behan, X. Wang, A. Butturini, V. I. Avramis, S. D. Mittelman, Adipocytes cause leukemia cell resistance to L-asparaginase via release of glutamine. *Cancer Res.* **73**, 2998–3006 (2013).
19. H. Li, S. Ning, M. Ghandi, G. V. Kryukov, S. Gopal, A. Deik, A. Souza, K. Pierce, P. Keskula, D. Hernandez, J. Ann, D. Shkoza, V. Apfel, Y. Zou, F. Vazquez, J. Barretina, R. A. Pagliarini, G. G. Galli, D. E. Root, W. C. Hahn, A. Tsherniak, M. Giannakis, S. L. Schreiber, C. B. Clish, L. A. Garraway, W. R. Sellers, The landscape of cancer cell line metabolism. *Nat. Med.* **25**, 850–860 (2019).
20. J. Zhang, N. N. Pavlova, C. B. Thompson, Cancer cell metabolism: The essential role of the nonessential amino acid, glutamine. *EMBO J.* **36**, 1302–1315 (2017).
21. M. Gangolf, J. Czerniecki, M. Radermecker, O. Detry, M. Nisolle, C. Jouan, D. Martin, F. Chantraine, B. Lakaye, P. Wins, T. Grisar, L. Bettendorff, Thiamine status in humans and content of phosphorylated thiamine derivatives in biopsies and cultured cells. *PLOS ONE* **5**, e13616 (2010).
22. W. Weber, H. Kewitz, Determination of thiamine in human plasma and its pharmacokinetics. *Eur. J. Clin. Pharmacol.* **28**, 213–219 (1985).
23. S. Dhir, M. Tarasenko, E. Napoli, C. Giulivi, Neurological, psychiatric, and biochemical aspects of thiamine deficiency in children and adults. *Front. Psych.* **10**, 207 (2019).
24. S. A. Romanski, M. M. McMahon, Metabolic acidosis and thiamine deficiency. *Mayo Clin. Proc.* **74**, 259–263 (1999).
25. S. Shah, E. Wald, Type B lactic acidosis secondary to thiamine deficiency in a child with malignancy. *Pediatrics* **135**, e221–e224 (2015).
26. A. Blackman, A. Boutin, A. Shimanovsky, W. J. Baker, N. Forcello, Levocarnitine and vitamin B complex for the treatment of pegaspargase-induced hepatotoxicity: A case report and review of the literature. *J. Oncol. Pharm. Pract.* **24**, 393–397 (2018).
27. C. R. Rausch, S. Paul, K. R. Marx, E. Jabbour, N. Pemmaraju, A. Ferrajoli, H. Kantarjian, L-carnitine and vitamin B complex for the treatment of pegasparaginase-induced hyperbilirubinemia. *Clin. Lymphoma Myeloma Leuk.* **18**, e191–e195 (2018).
28. I. Bairati, F. Meyer, E. Jobin, M. Gélinas, A. Fortin, A. Nabid, F. Brochet, B. Têtu, Antioxidant vitamins supplementation and mortality: A randomized trial in head and neck cancer patients. *Int. J. Cancer* **119**, 2221–2224 (2006).
29. B. D. Lawenda, K. M. Kelly, E. J. Ladas, S. M. Sagar, A. Vickers, J. B. Blumberg, Should supplemental antioxidant administration be avoided during chemotherapy and radiation therapy? *J. Natl. Cancer Inst.* **100**, 773–783 (2008).
30. C. B. Ambrosone, G. R. Zirpoli, A. D. Hutson, W. E. McCann, S. E. McCann, W. E. Barlow, K. M. Kelly, R. Cannioto, L. E. Sucheston-Campbell, D. L. Hershman, J. M. Unger, H. C. F. Moore, J. A. Stewart, C. Isaacs, T. J. Hobday, M. Salim, G. N. Hortobagyi, J. R. Gralow, G. T. Budd, K. S. Albain, Dietary supplement use during chemotherapy and survival outcomes of patients with breast cancer enrolled in a cooperative group clinical trial (SWOG S0221). *J. Clin. Oncol.* **38**, 804–814 (2020).
31. M. Harvie, Nutritional supplements and cancer: Potential benefits and proven harms. *Am. Soc. Clin. Oncol. Educ. Book* **2014**, e478–e486 (2019).
32. C. M. Velicer, C. M. Ulrich, Vitamin and mineral supplement use among US adults after cancer diagnosis: A systematic review. *J. Clin. Oncol.* **26**, 665–673 (2008).
33. G. R. Zirpoli, P. M. Brennan, C.-C. Hong, S. E. McCann, G. Ciupak, W. Davis, J. M. Unger, G. T. Budd, D. L. Hershman, H. C. Moore, J. Stewart, C. Isaacs, T. Hobday, M. Salim, G. N. Hortobagyi, J. R. Gralow, K. S. Albain, C. B. Ambrosone, Supplement use during an intergroup clinical trial for breast cancer (S0221). *Breast Cancer Res. Treat.* **137**, 903–913 (2013).
34. A. Nakamura, T. Nambu, S. Ebara, Y. Hasegawa, K. Toyoshima, Y. Tsuchiya, D. Tomita, J. Fujimoto, O. Kurasawa, C. Takahara, A. Ando, R. Nishigaki, Y. Satomi, A. Hata, T. Hara, Inhibition of GCN2 sensitizes ASNS-low cancer cells to asparaginase by disrupting the amino acid response. *Proc. Natl. Acad. Sci. U.S.A.* **115**, E7776–E7785 (2018).
35. L. K. Pino, B. C. Searle, J. G. Bollinger, B. Nunn, B. MacLean, M. J. MacCoss, The Skyline ecosystem: Informatics for quantitative mass spectrometry proteomics. *Mass Spectrom. Rev.* **39**, 229–244 (2020).
36. K. Birsoy, T. Wang, W. W. Chen, E. Freinkman, M. Abu-Remaileh, D. M. Sabatini, An essential role of the mitochondrial electron transport chain in cell proliferation is to enable aspartate synthesis. *Cell* **162**, 540–551 (2015).
37. X. G. Zhu, S. Nicholson Puthenveedu, Y. Shen, K. La, C. Ozlu, T. Wang, D. Klompstra, Y. Gultekin, J. Chi, J. Fidelin, T. Peng, H. Molina, H. C. Hang, W. Min, K. Birsoy, CHP1 regulates compartmentalized glycerolipid synthesis by activating GPAT4. *Mol. Cell* **74**, 45–58.e7 (2019).
38. R. A. Weber, F. S. Yen, S. P. V. Nicholson, H. Alwaseem, E. C. Bayraktar, M. Alam, R. C. Timson, K. La, M. Abu-Remaileh, H. Molina, K. Birsoy, Maintaining iron homeostasis is the key role of lysosomal acidity for cell proliferation. *Mol. Cell* **77**, 645–655.e7 (2020).
39. J. Garcia-Bermudez, L. Baudrier, E. C. Bayraktar, Y. Shen, K. La, R. Guarecuco, B. Yucel, D. Fiore, B. Tavora, E. Freinkman, S. H. Chan, C. Lewis, W. Min, G. Inghirami, D. M. Sabatini, K. Birsoy, Squalene accumulation in cholesterol auxotrophic lymphomas prevents oxidative cell death. *Nature* **567**, 118–122 (2019).
40. M. Ghandi, F. W. Huang, J. Jané-Valbuena, G. V. Kryukov, C. C. Lo, E. R. McDonald III, J. Barretina, E. T. Gelfand, C. M. Bielski, H. Li, K. Hu, A. Y. Andreev-Drakhlin, J. Kim, J. M. Hess, B. J. Haas, F. Aguet, B. A. Weir, M. V. Rothberg, B. R. Paolella, M. S. Lawrence, R. Akbani, Y. Lu, H. L. Tiv, P. C. Gokhale, A. de Weck, A. A. Mansour, C. Oh, J. Shih, K. Hadi, Y. Rosen, J. Bistline, K. Venkatesan, A. Reddy, D. Sonkin, M. Liu, J. Lehar, J. M. Korn, D. A. Porter, M. D. Jones, J. Golji, G. Caponigro, J. E. Taylor, C. M. Dunning, A. L. Creech, A. C. Warren, J. M. McFarland, M. Zamanighomi, A. Kauffmann, N. Stransky, M. Imielinski, Y. E. Maruvka, A. D. Cherniack, A. Tsherniak, F. Vazquez, J. D. Jaffe, A. A. Lane, D. M. Weinstock, C. M. Johannessen, M. P. Morrissey, F. Stegmeier, R. Schlegel, W. C. Hahn, G. Getz, G. B. Mills, J. S. Boehm, T. R. Golub, L. A. Garraway, W. R. Sellers, Next-generation characterization of the Cancer Cell Line Encyclopedia. *Nature* **569**, 503–508 (2019).

Acknowledgments: We thank all the members of the Birsoy laboratory for helpful suggestions. We also thank the Genomics Resource Center and Comparative Bioscience Center at Rockefeller University for support on genomic and animal studies, respectively. **Funding:** This research was supported by the NIH (DP2CA228042-01 to K.B.) and Chapman-Perelman MMRF grant (to K.B.). This study was also supported by a grant from the STARR Cancer Consortium. K.B. is also a Sidney Kimmel, Pew-Stewart, and Searle Scholar. K.B. serves as a consultant for Nanocare Technologies. R.G., R.T.W., and M.C.P. were supported by a Medical Scientist Training Program grant from the National Institute of General Medical Sciences of the National Institutes of Health under award number T32GM007739 to the Weill Cornell/Rockefeller/Sloan Kettering Tri-Institutional MD-PhD Program. R.T.W. and M.C.P. were also supported by F30/F31 Predoctoral Fellowships from the National Cancer Institute under award numbers 1F30CA247199-01 and F30CA247026-01, respectively. K.L. was also supported by an F31 Predoctoral Fellowship from the National Cancer Institute under award number 7F31CA247528-02. J.G.-B. is a Special Fellow of the Leukemia and Lymphoma Society. **Author contributions:** K.B. and R.G. conceived the project and designed the experiments. R.G. performed most of the experiments. R.T.W., L.B., N.E., and M.M. assisted with the cell competition experiments. K.L. performed computational analysis. H.A., B.R., J.F., and H.M. performed the metabolite profiling experiments. R.T.W., L.B., M.C.P., and J.G.-B. assisted with the mouse xenograft experiments. K.B. and R.G. wrote and edited the manuscript. **Competing interests:** The authors declare that they have no competing interests. **Data and materials availability:** All data needed to evaluate the conclusions in the paper are present in the paper and/or the Supplementary Materials. All supporting data and materials generated in this study can be requested from and will be fulfilled by the corresponding author.

Submitted 10 May 2020
Accepted 18 August 2020
Published 9 October 2020
10.1126/sciadv.abc7120

Citation: R. Guarecuco, R. T. Williams, L. Baudrier, K. La, M. C. Passarelli, N. Ekizoglu, M. Mestanoglu, H. Alwaseem, B. Rostandy, J. Fidelin, J. Garcia-Bermudez, H. Molina, K. Birsoy, Dietary thiamine influences L-asparaginase sensitivity in a subset of leukemia cells. *Sci. Adv.* **6**, eabc7120 (2020).